

DETAILED MATERIALS AND METHODS

HCV RNA, Genotype and HCV-Antibody Testing

Qualitative HCV-RNA testing was performed using COBAS Ampliprep/COBAS Amplicor HCV Test, version 2.0 (Roche Molecular Systems, Inc., Branchburg, NJ) (sensitivity 50 IU/ml). HCV genotyping was performed as previously described¹ as part of the clinical follow-up of patients. Presence of anti-HCV antibodies was assessed by the AxSym HCV Assay (Abbott GMBH & CO, K.G.).

IFN γ ELISPOT assay

HCV-specific T cell responses were measured using an IFN γ ELISPOT assay as previously described², with an input of 2×10^5 PBMCs /well against 10 pools of overlapping peptides spanning the entire HCV polyprotein. Peptides were corresponding to the HCV genotype 1a (H77) and genotype 1b (J4) sequences (BEI Resources, Manassas, VA). All assays were performed directly ex vivo on frozen PBMCs. Specific Spot forming cells (SFC) were calculated as “mean number of spots in test wells – mean number of spots in negative control wells” and normalized to SFC/ 10^6 PBMCs. A response was scored positive if greater than 50 SFC/ 10^6 PBMCs.

Peptides and HLA Class I Tetramers

Peptides were synthesized by Sheldon Biotechnology Centre, McGill University (Montreal, QC, Canada). MHC class I tetramers were synthesized by the National Immune Monitoring Laboratory (NIML), (Montréal, QC, Canada) or the NIH Tetramer Core Facility (Emory University, Atlanta, GA) and are as follows: HLA-A1 restricted

HCV NS3 peptide amino acids (aa) 1436–1444 (ATDALMTGY) [A1/NS3-1436], HLA-A2 restricted HCV NS3 peptide aa 1073–1081 (CINGVCWTV) [A2/NS3-1073], HLA-B27 restricted HCV peptide NS5B peptide aa 2841-2849 (ARMILMTHF) [B27/NS5B-2841].

Flow cytometry Antibodies

Directly conjugated antibodies against the following molecules were used: CD3-Alexa Fluor® 700 or –FITC (clone UCHT1), CD4-Pacific Blue™ or –PE or –FITC (clone RPA-T4), CD8-Alexa Fluor® 700 or –Pacific Blue™ (clone RPA-T8), CD8-APC-H7 (clone SK1), CD27-APC-H7 (clone M-T271), CD279/PD-1-APC (clone MIH4), CD244/2B4-FITC (clone 2-69), IFN γ -APC (clone B27), IL-2-PE (MQ1-17H12), TNF α -Alexa Fluor® 700 (clone MAb11) and CD107a/LAMP-1-PE-Cy™ 5 (clone H4A3) all from BD Biosciences, San Diego, CA; CD3-ECD (clone UCHT1) and CD8-ECD (clone SFC121Thy2D3) from Beckman Coulter, Marseille, France; CD127/IL-7Ra-eFluor®450 (clone eBioRDR5) from eBioscience, San Diego, CA; Tim3-PerCP (clone 344823) from R&D Systems Inc., San Diego, CA). Live cells were identified using Aqua Live/Dead fixable dead cell Stain Kit (Life Technologies, Burlington, ON). Fluorescence minus one (FMO) control stains were used to determine background levels of staining. Multiparameter flow cytometry was performed using a standard BD LSR II instrument equipped with blue (488 nm), red (633 nm), and violet (405 nm) lasers (BD Biosciences,) using FACSDiva software version 6.1.3 (BD Biosciences). Data files were analyzed using FlowJo software version 9.4.11 for Mac (Tree Star, Inc., Ashland, OR).

Phenotypic and functional analysis of HCV-specific T cells

All assays were performed on archived frozen PBMCs. Tetramer staining for CD8-specific T cells was performed as previously described³ using the listed panel of tetramers. Intracellular cytokine staining (ICS) and CD107a degranulation assay were performed as previously described³ in response to HCV peptide pool (1 µg/ml) or HCV minimum peptide (10 µg/ml) or SEB (200 ng/ml) as a positive control. Polyfunctionality was assessed by exporting flow cytometry standard (FCS) data as Boolean gates using FlowJo (version 9.5) and SPICE software⁴. Carboxyfluorescein succinimidyl ester (CFSE) proliferation assays were performed as previously described³ in a 6 day proliferation assay with or without HCV minimum-peptide or peptide pool (final concentration 1 µg/ml). Recombinant human IL-2 (20 IU/ml) (NIH AIDS Research and Reference Reagent Program, ATCC, Manassas, VA) was added 3 days post stimulation.

HCV Epitope Sequencing

HCV RNA was extracted from EDTA plasma using AxyPrep Body Fluid Viral DNA/RNA Miniprep Kit (Axygen, Union City, CA) according to the manufacturer's protocol. HCV RNA was reverse transcribed and PCR amplified by sets of nested primers specific for epitopes NS3-1073 and NS3-1436 as previously described³. PCR products were purified and cloned in pCR 4-Topo (Life Technologies) using the Topo TA cloning kit for sequencing (Life Technologies) and sequenced at the Molecular Biology and Functional Genomics service of the Institut de Recherches Cliniques de Montréal (IRCM) (Montreal, QC).

Functional avidity assays

Functional avidity of epitope specific CD8 T cells was measured as the dose-dependent production of IFN γ in response to stimulation by the reference and variant epitope sequences in an IFN- γ ELISPOT assay, as previously described ⁵.

Statistical Analysis

Statistical analysis for ELISPOT results was performed with GraphPad Prism 5 using one-tailed Mann-Whitney test at a confidence interval of 90%.

References

1. Murphy DG, Willems B, Deschenes M, et al. Use of sequence analysis of the NS5B region for routine genotyping of hepatitis C virus with reference to C/E1 and 5' untranslated region sequences. *J Clin Microbiol* 2007;45:1102-12.
2. Pelletier S, Drouin C, Bedard N, et al. Increased degranulation of natural killer cells during acute HCV correlates with the magnitude of virus-specific T cell responses. *J Hepatol* 2010;53:805-16.
3. Badr G, Bedard N, Abdel-Hakeem MS, et al. Early interferon therapy for hepatitis C virus infection rescues polyfunctional, long-lived CD8+ memory T cells. *J Virol* 2008;82:10017-31.
4. Roederer M, Nozzi JL, Nason MC. SPICE: exploration and analysis of post-cytometric complex multivariate datasets. *Cytometry A* 2011;79:167-74.
5. Abdel-Hakeem MS, Bedard N, Badr G, et al. Comparison of immune restoration in early versus late alpha interferon therapy against hepatitis C virus. *J Virol* 2010;84:10429-35.

Supplementary Table S1: Patients' characteristics and demographics

Patient code	Status at start of follow-up	Age at reinfection (years)	Gender	Duration of injection (years)	No of Injections during past month ^a	Serum ALT during early reinfection ^b (U/L)	HCV Genotype (First infection/ Second infection)	HLA Class I	Reactive Tetramers
SR/SR-1	HCV Resolver	53	M	13.4	> 30	3090	ND/1	A2, B58	A2/NS3-1073 A2/NS5B-2594
SR/SR-2	HCV Resolver	43	M	15.4	≤ 30	25	ND/1	A24/A26, B27/B49	B27/NS5B-2841
SR/SR-3	HCV Naïve	42	M	14.4	> 30	23	1a/1	A23/A32 B27/B44	B27/NS5B-2841
SR/SR-4	Early reinfection	36	F	12.3	≤ 30	15	ND/1	A2/A24 B7/B39	A2/NS3-1073
SR/SR-5	Early reinfection	44	M	31.5	> 30	183	ND/1a	A2/A23 B18/B49	None
SR/CI-1	HCV Naïve	28	M	6.1	> 30	88	ND/1a	A1 /A3 B44/B49	A1/NS3-1436
SR/CI-2	Acute primary HCV	29	M	1.1	≤ 30	17	1a/1a	A2, B39/B44	A2/NS3-1073
SR/CI-3	HCV Resolver	30	F	4.1	≤ 30	42	ND/1a	A1/A29 B35/B44	A1/NS3-1436
SR/CI-4	Early reinfection	33	M	3	> 30	20	ND/1b	A2, B44/B51	A2/NS3-1073

ND = Not determined; SR: Spontaneous Resolution; CI: Chronic Infection

^a A strong and independent predictor of HCV incidence in this cohort (Bruneau J et al, Addiction. 2012 Jul;107(7):1318-27)

^b at < 4 wks

SUPPLEMENTARY FIGURE LEGENDS

Supplementary Figure S1: Lack of expansion of HCV-specific T cells in patient SR/SR-3 upon reinfection, is due to being infected by a different HCV subtype. Results from longitudinal ELISPOT assays for patient SR/SR-3 where PBMCs were stimulated with overlapping peptide pools representing the entire HCV genome for (A) genotype 1a and (B) genotype 1b. The dashed lines delineate the different infection episodes. Responses to genotype 1b peptide pools during the reinfection episode for patients with genotype 1 and an unknown subtype SR/SR-1 (C), SR/SR-4 (D) and SR/CI-4 (E). BDL = Below detection level.

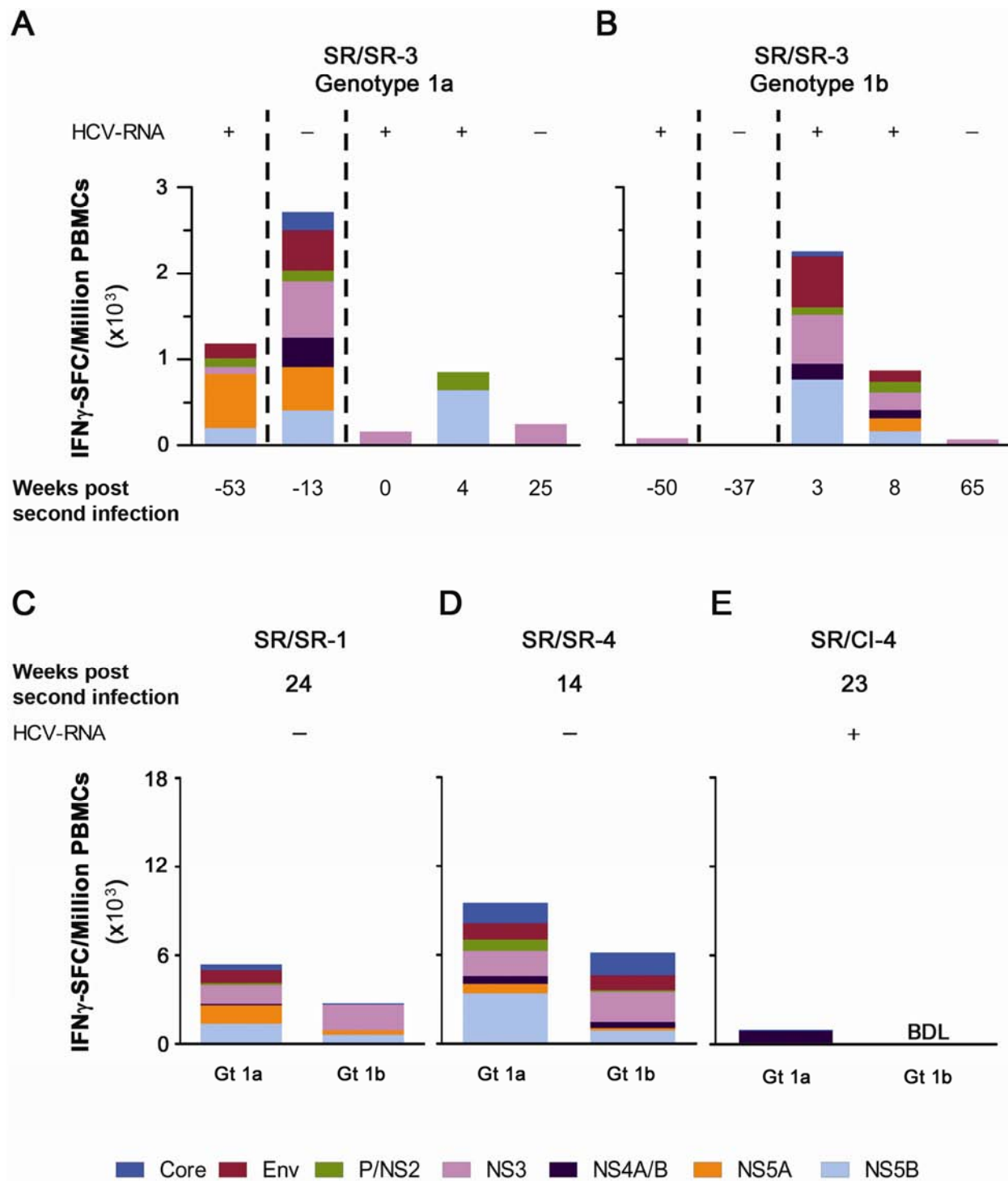
Supplementary Figure S2: Higher proliferative capacity for HCV-specific CD4 and CD8 T cells in SR/SR patients in comparison to SR/CI patients. Proliferation of HCV-specific CD4 and CD8 T cells was assessed in a 6-day CFSE proliferation assay against a panel of overlapping peptide pools representing the immunodominant regions of HCV (NS3 and NS5B) and HCV regions showing the highest response in the IFN γ ELISPOT assay. Representative dot plots showing the proliferation indicated by the percentage of CFSE^{lo} cells from patient SR/SR-4 (A) non-stimulated versus (B) stimulated with peptide pool NS3-1 (NS3 aa: 1016-1341) and patient SR/CI-3 (C) non-stimulated versus (D) stimulated with peptide pool P7/NS2 (P7/NS2 aa: 743-1026). The cells were gated on viable CD3⁺ then CD4⁺ or CD8⁺ T lymphocytes. The percentage of proliferating cells is shown on the left of the histograms (upper panels) and on the dot plots (lower panels).

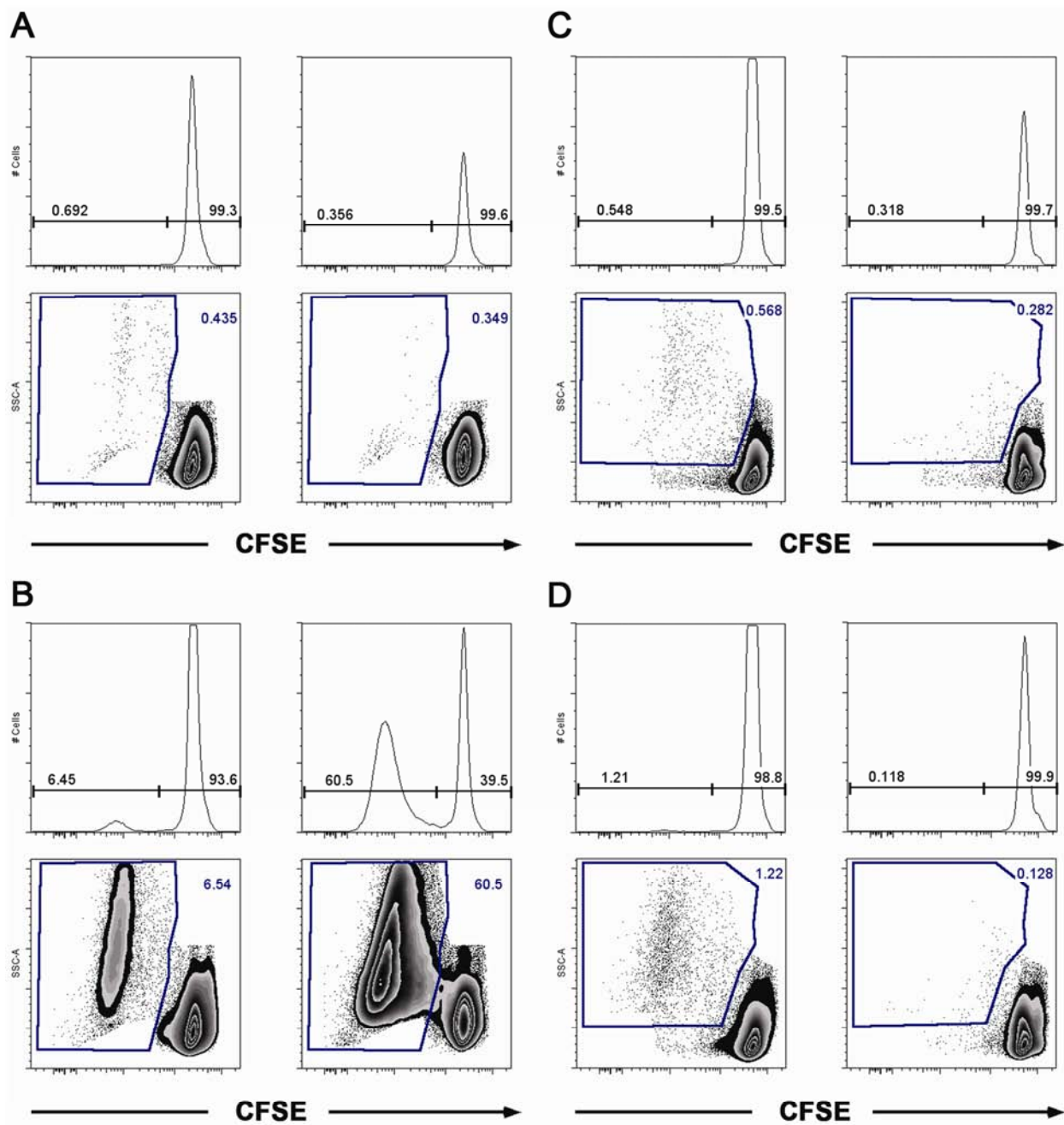
Supplementary Figure S3: Higher production of cytokines/CD107a expression by HCV-specific CD8 T cells in patients from SR/SR group in comparison to patients from SR/CI group. (A) Gating strategy. Representative dot plots from (B) patient SR/SR-4 and (C) patient SR/CI-2 showing the production of cytokines (IFN γ , IL-2 and TNF α) and the expression of CD107a in response to stimulation with peptide pools representing NS5B-1 and NS3-1, respectively, gated on viable CD8⁺ CD3⁺ T lymphocytes.

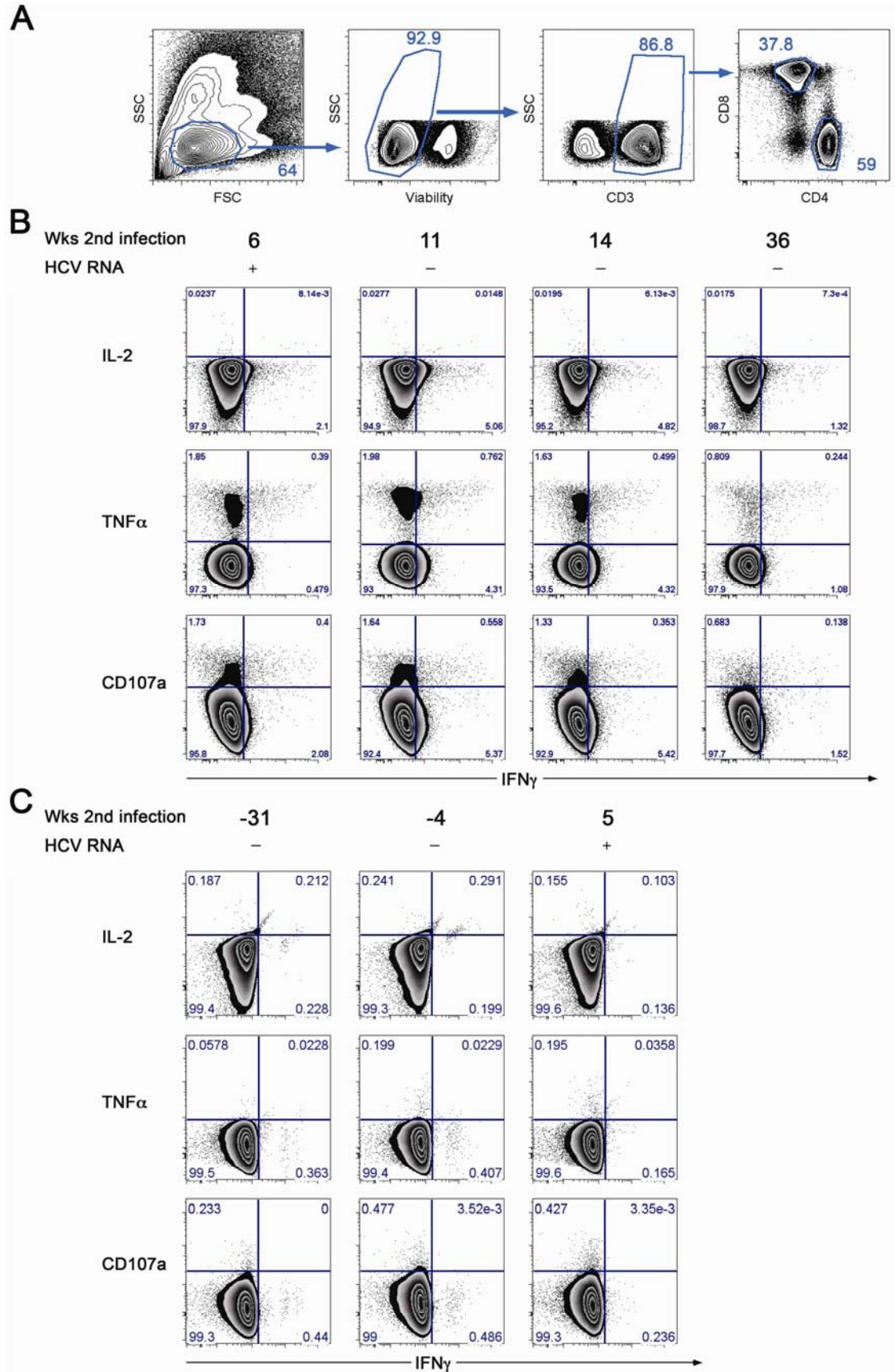
Supplementary Figure S4: No significant changes in CD27 or the exhaustion markers Tim3 or CD244 (2B4) in either of the 2 groups of patients. Representative dot plots for phenotyping of

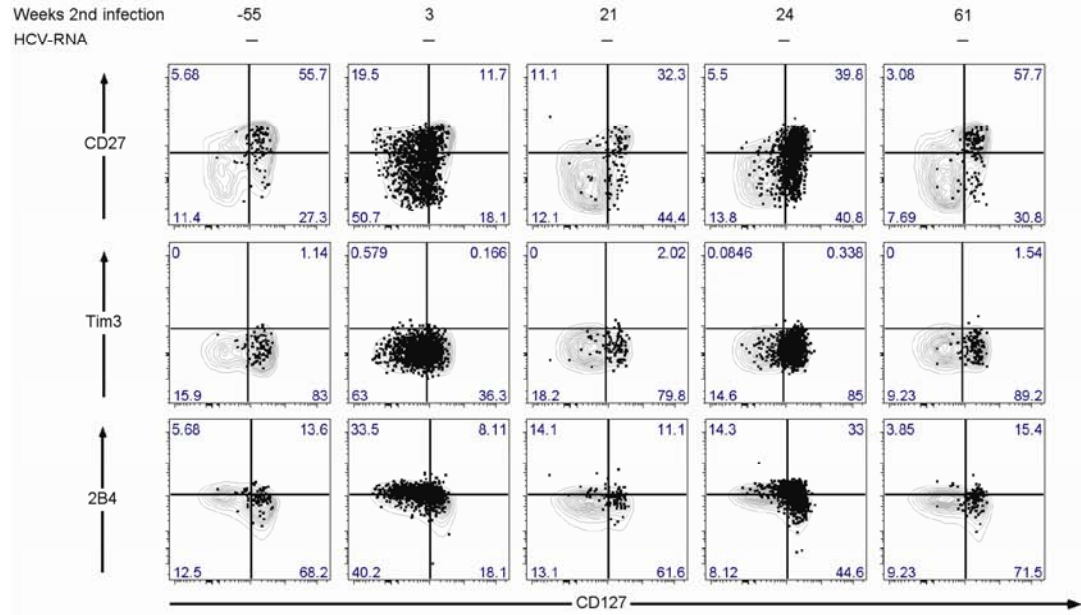
(A) patient SR/SR-1 with A2/NS3-1073 tetramer and (B) patient SR/CI-1 with A1/NS3-1436 tetramer, showing the expression of CD27, Tim3 and 2B4 on tetramer+ cells. The black dots represent the tetramer+ HCV-specific CD8+ T cells overlaid on the grey contour plots representing total CD3+ CD8+ T cells in the same patient. Percentages of expression on tetramer+ cells are shown in each quadrant.

Supplementary Figure S5: Shift in immunological dominance of the targeted epitope between the primary infection and the reinfection episode in patient SR/SR-1. Dot plots for longitudinal tetramer staining (upper panel) and phenotyping (lower panel) from patient SR/SR-1 with A2/NS5B-2594 tetramer gated on viable CD3+ T lymphocytes. The A2/NS5B-2594 tetramer+ population expanded higher frequencies than the A2/NS3-1073 tetramer+ cells that were present at a higher frequency post the primary infection (**Figure 5A and 5C**).







A**B**